Homoleptic Cu-phosphorus and Cu-ethene complexes.

Gustavo Santiso-Quiñones*, Andreas Reisinger, John Slattery, and Ingo Krossing.*[a]

Supplemental Material

General considerations based on Born-Fajans-Haber cycles and theoretical calculations:

The simplest approach to Cu^I salts of WCAs ($[A]^-$) would certainly be a metathesis reaction from either a Li or Ag salt (scheme S.1).

$$\begin{tikzcd}
& Li^+_{(g)} + [A]^-_{(g)} + Cu^+_{(g)} + X^-_{(g)} \arrow[dr, "\begin{array}{l}- \Delta_{Latt}H(Cu[A]) \\ - \Delta_{Latt}H(LiX)\end{array}"] & \\
Li[A]_{(s)} + CuX_{(s)} \arrow[ur, "\begin{array}{l}+ \Delta_{Latt}H(Li[A]) \\ + \Delta_{Latt}H(CuX)\end{array}"] \arrow[rr, "\Delta_rH_{(s)}"] & & Cu[A]_{(s)} + LiX_{(s)}
\end{tikzcd}$$

Scheme S.1. Born-Fajans-Haber cycle for the metathesis reaction leading to $Cu[Al(pftb)_4]$, pftb = $OC(CF_3)_3$, A = Anion, X = Halide.

Since the (estimated) lattice energies of all ligand-free alkoxyaluminate salts differ by approximately only 10 kJ mol^{-1}, $\Delta H_{Latt}(Li[A])$ and $\Delta H_{Latt}(Cu[A])$ cancel in a 0th order approach. The resulting enthalpy can be estimated according to eq. **(s.i)**

$$\Delta_rH_{(s)} \approx \Delta H_{Latt}(CuX) - \Delta H_{Latt}(LiX) \qquad \textbf{(s.i)}$$

Unfortunately, the enthalpy Δ_rH is positive for Cl (132 kJ mol^{-1}), Br (158 kJ mol^{-1}) and I (200 kJ mol^{-1}) and the reaction is unlikely to proceed. If Li is changed for Ag, Δ_rH becomes less positive (78 (Cl), 73 (Br) and 74 (I) kJ mol^{-1}), but still no reaction would be expected. To overcome this problem, one has to supply an additional gain in energy. This energy can be delivered, if a salt of a silver complex is used instead of the ligand free $Ag[Al(pftb)_4]$ according to scheme S.2.

Again, the lattice enthalpies of the aluminate salts cancel, however, the resulting enthalpy for the exchange of the metal is now described according to eq. **(s.ii)**:

$$\Delta_rH_{(s)} \approx \Delta H_{Latt}(AgX) - \Delta H_{Latt}(CuX) + \Delta_rH_{(g)} \qquad \textbf{(s.ii)}$$

For a successful reaction, the absolute value of $\Delta_rH_{(g)}$ has to be bigger than the absolute value of the difference $\Delta H_{Latt}(AgX)$ - $\Delta H_{Latt}(CuX)$. Since the complexation enthalpies for Ag are the smallest of all coinage metals,[s.1] the method sketched here holds for a variety of Cu^I complexes.

$$\begin{tikzcd}
AgL_n^+{}_{(g)} + [A]^-_{(g)} + Cu^+_{(g)} + I^-_{(g)} \arrow[r, "\Delta_rH_{(g)}"] & Ag^+_{(g)} + I^-_{(g)} + CuL_n^+{}_{(g)} + [A]^-_{(g)} \arrow[d, "\begin{array}{l}- \Delta_{Latt}H(CuL_n[A]) \\ - \Delta_{Latt}H(AgI)\end{array}"] \\
AgL_n[A]_{(s)} + CuI_{(s)} \arrow[u, "\begin{array}{l}+ \Delta_{Latt}H(AgL_n[A]) \\ + \Delta_{Latt}H(CuI)\end{array}"] \arrow[r, "\Delta_rH_{(s)}"] & CuL_n[A]_{(s)} + AgI_{(s)}
\end{tikzcd}$$

Scheme S.2. Born-Fajans-Haber cycle for the metathesis reaction leading to $CuL_n[Al(pftb)_4]$, pftb = $OC(CF_3)_3$, L = Ligand, A = Anion, X = Halide. $\Delta H_{(latt)}(CuI)$ = 966 kJ mol^{-1} and $\Delta H_{(latt)}(AgI)$ = 889 kJ mol^{-1}.[s.2]

Values of $\Delta_rH_{(g)}$ for these isodesmic reactions in the gas phase can be calculated easily and in high accuracy (at the pbe0/TZVPP or MP2/TZVPP level). In Table S.1 ligand-exchange enthalpies $\Delta_rH_{(g)}$ as well as the resulting solid-state enthalpies $\Delta_rH_{(s)}$ for selected ligands are summarized.

Table S.1. Calculated ligand-exchange enthalpies $\Delta_rH_{(g)}$ and total enthalpies $\Delta_rH_{(s)}$ for the reaction assessed in scheme S.2.

L	n	$[Cu(L)_n]^+$	
		$\Delta_rH_{(g)}$	$\Delta_rH_{(s)}$
P_4[a]	2	-85	-8
C_2H_4[a]	3	-93	-17
C_2H_2[b]	4	-87	-13

[a] pbe0/TZVPP. [b] taken from ref. s.4a.

From table S.1 it is evident that the addition of a ligand to the system lowers the enthalpy ($\Delta_rH_{(s)}$) of the overall reaction and the negative values obtained suggest that a metathesis between Cu^+ and Ag^+ might be possible. Experimentally, we have shown that to be the case for the two novel complexes: $[Cu(\eta^2\text{-}P_4)_2][Al(OC(CF_3)_3)_4]$ and $[Cu(\eta^2\text{-}C_2H_4)_3][Al(OC(CF_3)_3)_4]$. The acetylene complex has not been synthesized yet, but from the experimental evidence obtained so far, the same experimental procedure should be promising.

Crystallization Procedures for $[Cu(P_4)_2]^+$ and $[Cu(C_2H_4)_3]^+$:

For the phosphorus complex crystals suitable for X-ray diffraction were grown from the mother liquid by reducing very slowly (c.a. 1-2 ml/30 min) the volume of the solution under vacuum until an oily solution remained. The oily solution was further evacuated at an even slower rate (c.a. 0.5 ml/h) until crystalline material started to form.

For the ethene complex, just by letting the flask stand at room temperature crystalline material precipitates out of the solution.

---

[a] *Albert-Ludwig Universität Freiburg.*
Institut für Anorganische und Analytische Chemie.
Albertstr. 21, 79104, Freiburg, Germnany.
Fax: +49-761-203-6122; Tel: +49-761-203-6001;
E-mail: gustavo.santiso@ac.uni-freiburg.de; krossing@uni-freiburg.de

Low temperature crystallization (c. a. 0°C) of the same mother liquid affords better crystals.

Overall crystal structures of [Cu(η^2-P_4)$_2$][Al(OC(CF_3)$_3$)$_4$] and [Cu(η^2-C_2H_4)$_3$][Al(OC(CF_3)$_3$)$_4$]:

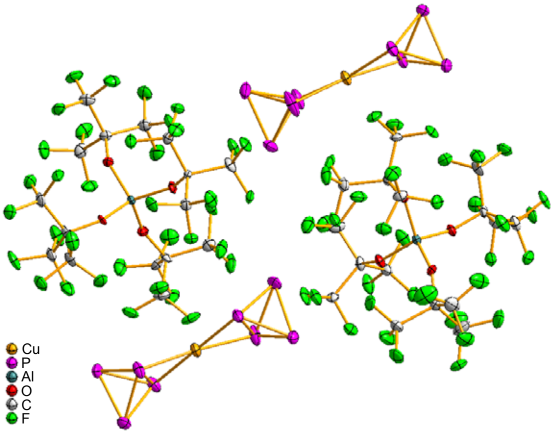

Figure S.1. Crystal structure of [Cu(η^2-P_4)$_2$][Al(OC(CF_3)$_3$)$_4$] showing the two independent ion pairs in the asymmetric unit. Thermal ellipsoids are drawn at 50% probability. Best view was chosen.

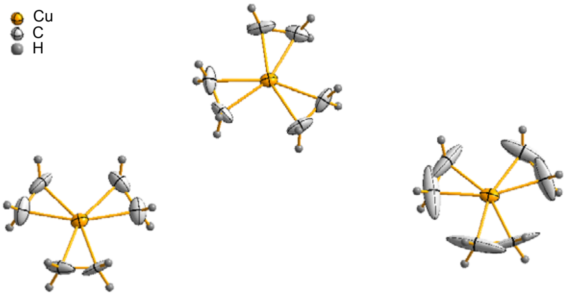

Figure S.2. Crystal structure of [Cu(η^2-C_2H_4)$_3$]$^+$ showing the three independent cations in the asymmetric unit. Thermal ellipsoids are drawn at 50% probability. For clarity all anions were omitted. Best view was chosen.

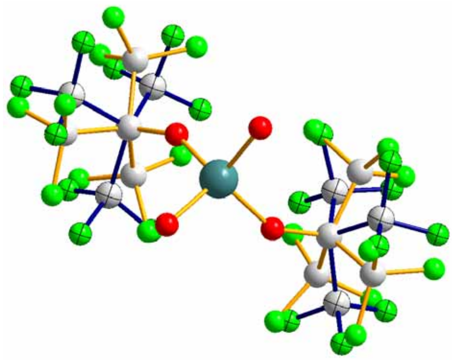

Figure S.3. Anion from the [Cu(η^2-C_2H_4)$_3$][Al(OC(CF_3)$_3$)$_4$] moiety showing the 2 disordered -(CF_3)$_3$ groups. For clarity the other two -C(CF_3)$_3$ rests were omitted. Disordered positions depicted with a different colour.

Data collection at different temperatures and refinement of the structure [Cu(C_2H_4)$_3$]$^+$:

For the ethene complex, depending on the temperature at which the data set is collected, different lattice parameters can be obtained.

At **173 K** only a small lattice can be found, namely a = 12.8455 Å, b = 14.9554 Å, c = 18.9665 Å, α = γ = 90° β = 102.505°, V = 3555.33 Å^3, which produces only one independent cation and anion. In this small lattice a disorder over three positions in the cation (namely the C_2H_4 groups) can be refined. The anion also shows some disordered -CF_3 groups. The final refinement gave a R1 value close to 9 %.

At 163 K one of the axes (a in this case) doubles (***a* = 25.9881 Å**, b = 14.9819 Å, c = 19.0157 Å, α = γ = 90° β = 98.389°, V = 7192.10 Å^3) and two independent cationic-anionic species can be refined. Still some disorder in the cations and anions was seen. The final R1 value was not better than the measurement at 173 K.

At 153 K the b axes triples (a = 12.8455 Å, ***b* = 44.8620 Å**, c = 18.9555 Å, α = γ = 90° β = 102.506°, V = 10664.39 Å^3) giving as a result three independent ionic pairs in the asymmetric unit. No disordered positions where found for the C_2H_4 moieties in either of the three independent species. A final R1 value of 7.27 % was obtained.

Attempts to collect a data set at 100 K failed due to an irreversible phase transition in the crystal. Even cooling down the crystal from 173 K to 100 K over a period of 10 h gave no reliable data sets. From all the data sets collected and refined, the unit cell with the largest axes (153 K, see above), which produces three cation-anion pairs in the asymmetric unit, seems to be a real crystallographic ordering of the molecules and not an artefact. Therefore, we have presented here the results of such a measurement.

Since the data set was collected at 153 K it was inevitable that thermal movement of the –CF_3 groups would be observed. This explains the relatively large thermal ellipsoids observed for some of the –CF_3 groups. The -C(CF_3)$_3$ groups are disordered by rotation around the C-O bond (see fig. S.3). This was modelled as two positions with a SOF ratio of 0.70/0.30 and refined using two free variables. SADI restraints were applied to the disordered groups. DFIX restraints for the C-F bond (1.34pm) were applied for one of the disordered groups. SIMU restraints were applied to one carbon atom (C_{38}). ISOR and DELU restraints were applied to 3 atoms, from the disordered residues, to correct for very asymmetric ADPs. The second disordered positions of the -CF_3´s with an SOF of 30 % were not refined anisotropically. All other atoms (except one F of the 108 fluorine atoms present) were successfully refined anisotropic. The structure refines to a satisfactory R1 (7.27 %) value and the description of the cation can be carried out.

For the cationic species, in two of the three independent units the thermal ellipsoids of the ethene ligands are relatively well described; in the third the thermal ellipsoids are rather diffuse (see figure S.2). For the two cationic units well described by their thermal parameters it could have been possible to refine the hydrogen atoms position, but the Uiso of some of them were smaller than the Ueq values of the carbon atoms to which they are bonded. Therefore, we decided to fix all hydrogen atoms by an AFIX command.

Weak P−F and Cu−F interaction for [Cu(P_4)$_2$]$^+$:

One of the independent $[Cu(P_4)_2]^+$ in the asymmetric unit is more symmetrical than the other due to the fact that it has on average weaker P−F interactions, i.e. the P−F distances are on average longer. These weak P−F and Cu−F interactions, attributed to crystal packing effects, are responsible for the non perfect D_{2h} symmetry observed in the cation (see figure S.4, cf. sum of the P and F van der Waals radii: 340 pm).[s.3]

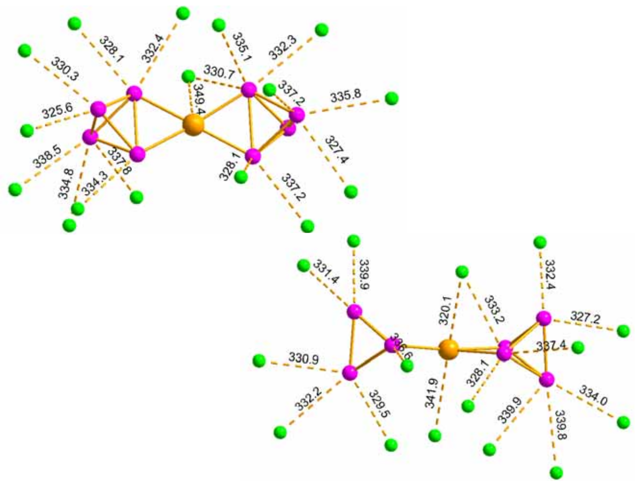

Figure S.4. P−F weak interactions below 340 pm and Cu−F between 320-349 pm in the two independent cations from $[Cu(P_4)_2][Al(OC(CF_3)_3)_4]$.

Weak F-H and Cu-F contacts in $[Cu(C_2H_4)_3]^+$

In $[Cu(C_2H_4)_3]^+$ there are three cation-anion pairs in the in the asymmetric unit. The weak H−F and Cu−F interactions are responsible for the non perfect D_{3h} symmetry observed in all of the cations (see figure S.5, cf. sum of the H and F Van der Waals radi: 290 pm).[s.3]

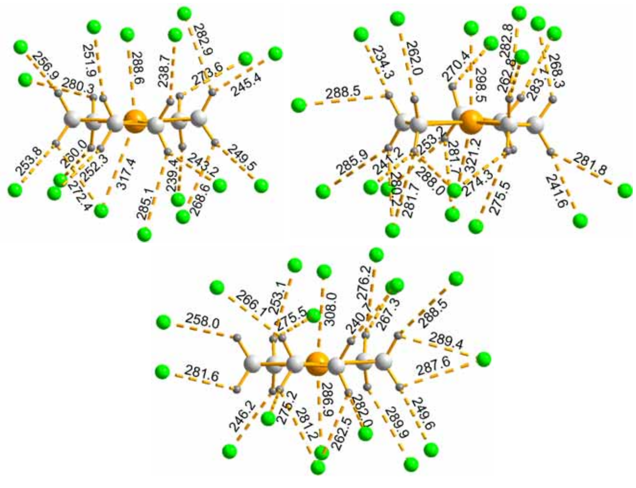

Figure S.5. H−F weak interactions below 290 pm and Cu−F between 287-321 pm in the three independent cations from $[Cu(C_2H_4)_3][Al(OC(CF_3)_3)_4]$. Arbitrary view for each cation was chosen.

The C=C Bond Distances of coordinated C_2H_4: X-ray Data vs. Stretching Frequency and Experiment vs. Theory

We have just submitted to *J. Am. Chem. Soc*.[s.4] a detailed description of the bonding in complexes of the type $[Ag(C_2H_4)_n]^+$ (n = 1-3) in which we include a method to extract the elongation of the C=C bond upon complexation to a metal. Here we present a summary of the most important aspects needed to apply this model to the $[Cu(C_2H_4)_3]^+$ system, a detailed description of this model can be found in reference s.4.

- The bond length of free gaseous ethene, derived from an analysis of the spectroscopic data, is known to be the most accurate available bond length (133.3 pm).

- Short C=C bond distances are often observed in the condensed phase (in X-ray crystallographic experiments) for metal-ethene complexes (e.g. $Ag(C_2H_4)_x$, x = 1 – 3). These short C=C distances, which may be shorter than the C=C distance in free ethene do not fit with the conventional view of bonding in metal-ethene complexes and are likey to be caused by systematic errors in the measurements.

- Factors such as temperature and high angle data play an important role in the description of the C=C bond length in the X-ray crystal structures of metal-ethene complexes. These effects cannot be corrected by the librational correction included in most programs for crystal structure solution and refinement and so contribute to the unexpectedly short C=C bond lengths that are observed.

- For various metal-ethene complexes of the general formula $M(\eta^2\text{-}C_2H_4)_n^{m+}$, the calculated (DFT: BP86/TZVPP, see ref. s.4) decrease (red shift) of the C=C stretching mode $\Delta\nu$ [cm^{-1}] may be plotted against the calculated (DFT: BP86/TZVPP, see ref. s.4) bond elongation Δd [pm] (both values relative to free ethene). From this plot, $\Delta\nu$ and Δd are seen to be proportional, with a proportionality constant of 26.8 $(cm\,pm)^{-1}$ (see figure S.6).

- This diagram generally holds for all weakly bound $M(\eta^2\text{-}C_2H_4)_n^{m+}$ complexes, unless the bond elongation is too large (> 4 pm) and the system is then better described as a metallacyclopropane.

- Using this correlation, it is possible to estimate $\Delta d_{spec.}$ for $[Cu(C_2H_4)_3]^+$ based on the experimental $\Delta\nu_{exp.}$ and the proportionality constant 26.8 $(cm\ pm)^{-1}$, as described by equation (iii)

$$\Delta d_{spec.} = (\Delta\nu_{exp.}/26.8)\ [pm] \qquad \textbf{(s.iii)}$$

- For our novel complex $[Cu(C_2H_4)_3]^+$ the observed vibrational frequency was 1577 cm^{-1} (see table s.2), the vibrational frequency of free ethene is 1623 cm^{-1}.[s.5] With these two values and using equation **(s.iii)**, Δd_{spec} is 1.7 pm. So based on Raman spectroscopy and with the aid of this methodology we would expect for our data set an elongation of the C=C bond with respect to free gaseous $H_2C{=}CH_2$ of 1.7 pm, i.e ≈ 135.0 pm.

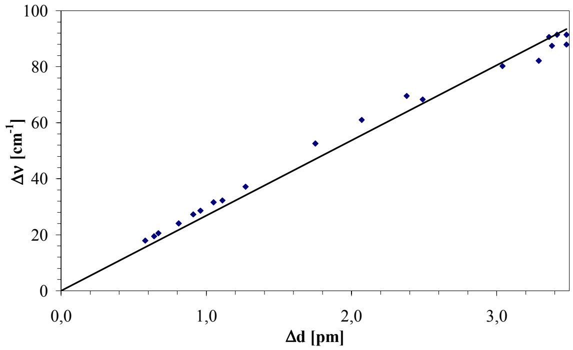

Figure S.5. Plot of the calculated stretching frequency decrease Δν [cm^{-1}] against the calculated bond elongation Δ*d* [pm] for various $M(C_2H_4)_n^y$ (n = 1 – 3, y = 0 (M = Ni, Pd, Pt) and 1 (M = Li, Na, K, Cu, Ag, Au) compounds. The slope of the line is 26.8 $(cm\ pm)^{-1}$ (see ref s.4)

d_{xz}-σ^*(P−P) interaction of symmetry orbitals in $[M(P_4)_2]^+$ (M = Cu, Ag), as described in ref. s.6

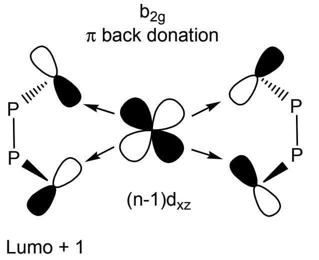

Raman spectra of $[Cu(\eta^2-P_4)_2][Al(OC(CF_3)_3)_4]$ and $[Cu(\eta^2-C_2H_4)_3][Al(OC(CF_3)_3)_4]$:

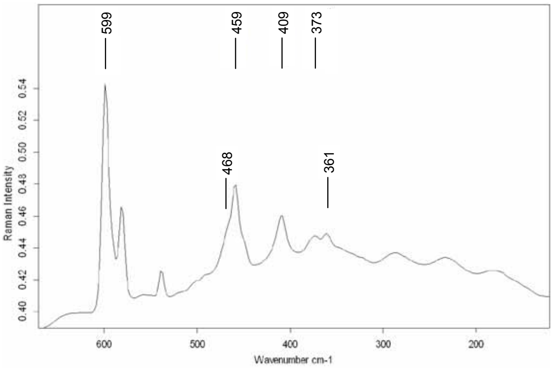

Figure S.7. Raman spectrum of $[Cu(\eta^2-P_4)_2][Al(OC(CF_3)_3)_4]$ from 650 – 100 cm^{-1}. The bands with labels correspond to the cation moiety, anion bands were not labelled, values given in table S.2.

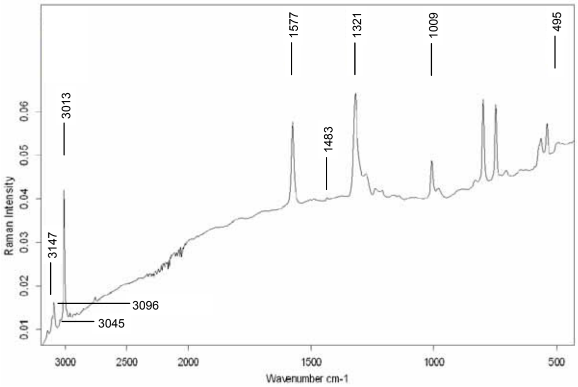

Figure S.8. Raman spectrum of $[Cu(\eta^2-C_2H_4)_3][Al(OC(CF_3)_3)_4]$. The bands with labels correspond to the cation moiety, anion bands were not labelled, values given in table S.2.

Table S.2. Experimental Raman bands[a] [cm^{-1}] for $[Cu(P_4)_2]$-$[Al(OC(CF_3)_3)_4]$ and $[Cu(C_2H_4)_3][Al(OC(CF_3)_3)_4]$. Comparison with the experimental bands of $[Ag(P_4)_2][Al(OC(CF_3)_3)_4]$[b] and $[Ag(C_2H_4)_3]$-$[Al(OC(CF_3)_3)_4]$.[c]

$Cu(P_4)_2^{+}$[d]	$Ag(P_4)_2^+$	$Cu(C_2H_4)_3^+$	$Ag(C_2H_4)_3^+$
95 (6)	-	122 (2)	-
183 (3)	-	171 (10)	-
-	-	-	216 (14)
233 (5)	-	238 (18)	235 (18)
286 (5)	-	291 (19)	287 (18)
-	322 (5)	324 (65)	322 (35)
-	-	369 (18)	-
361 (7)	**374 (9)**	-	-
373 (6)	**381 (sh)**	**-**	-
409 (20)	**413 (5)**	-	**409 (2)**
459 (37)	**458 (16)**	**495 (6)**	-
468 (19)	**473 (18)**	-	-
539 (12)	-	540 (25)	538 (22)
-	-	565 (18)	563 (17)
581 (45)	-	571 (14)	-
599 (100)	**601 (100)**	-	-
708 (5)	-	707 (6)	704 (3)
744 (5)	746 (7)	749 (58)	747 (46)
797 (8)	798 (7)	800 (65)	798 (54)
833 (5)	-	833 (5)	832 (4)
-	-	-	894 (2)
-	-	980 (7)	982 (12)
-	-	**1009 (29)**	**1002 (12)**
-	-	1089 (2)	1082 (2)
-	-	1143 (3)	1142 (2)
-	-	1170 (2)	1163 (2)
-	-	1212 (4)	-
-	-	1240 (5)	1239 (7)
-	-	1278 (16)	1275 (13)
-	-	**1321 (78)**	**1326 (100)**
-	-	**1438 (2)**	-
-	-	**1577 (65)**	**1585 (77)**
-	-	**3013 (100)**	**3010 (78)**
-	-	**3045 (4)**	-
-	-	**3096 (19)**	**3090 (19)**
-	-	**3147 (6)**	**3162 (4)**

[a] The bands corresponding to the cationic species are depicted with another color. [b] taken from ref. s.7. [c] taken from ref. s.4 (Just submited to *J. Am. Chem. Soc.*). [d] Bands above 850 cm^{-1} were not seen or have a very weak inteansity (< 2)

Experimental Section

All manipulations were carried out inside a glovebox under an N_2 atmosphere. $AgAl(OC(CF_3)_3)_4$ was synthesized according to reported procedures.[s.8] Commercially available CuI was used as supplied. P_4 (available in house) was purified by extraction and recrystallization from CS_2. Ethene (3.5, fma Linde) was used as supplied. The glassware (a modified Schlenk vessel) used for the reactions is depicted here.

$[Cu(P_4)_2][Al(OC(CF_3)_3)_4]$: $AgAl(OC(CF_3)_3)_4$ (0.5 g, 0.47 mmol), CuI (0.27 g, 1.40 mmol) and P_4 (0.12 g, 0.9 mmol) were introduced into a double Schlenk equipped with a G4 filter (see right). The flask was evacuated (10^{-3} mbar) and CH_2Cl_2 was condensed inside. The flask was put into an ultrasonic bath and the suspension was sonicated for 48 h. After sonication the sample was filtered to the other side of the Schlenk. With the aid of liquid N_2 the solvent was condensed back into the reaction side, the remaining material was washed, and the solution was filtered again. Crystallization of the sample was carried out (see description above). Colorless crystals (0.51 g, 0.40 mmol, 85 % yield) very sensitive to air and moisture which ignite spontaneously in air were isolated and characterized by NMR (CD_2Cl_2, -90 °C): ^{31}P-NMR: $\delta = -460$ ppm (s, 8P), ^{19}F-NMR: $\delta = -76.8$ ppm (s, 36F), ^{27}Al-NMR: $\delta = 34.8$ ppm (s, 1Al) and Raman spectroscopy [cm^{-1}/(%)] = 599(100), 468(19), 459(37), 409(20), 373(6), 361(7), and X-ray single crystal structure.

$[Cu(C_2H_4)_3][Al(OC(CF_3)_3)_4]$: $AgAl(OC(CF_3)_3)_4$ (1.16 g, 1.00 mmol) and CuI (0.571 g, 3.00 mmol) were inrtoduced into a double Schlenk equipped with a G4 filter (see right). The flask was evacuated (10^{-3} mbar) and CH_2Cl_2 was condensed inside. With the aid of liquid N_2, the solvent was frozen and the flask was evacuated again to 10^{-3} mbar. Using a metal line, C_2H_4 was added to the flask until the total pressure of the system reached 2-2.5 bar. The flask was put into an ultrasonic bath and the suspension was sonicated for 48 h. After sonication the sample was filtered to the other side of the Schlenk. With the aid of liquid N_2 the solvent was condensed back into the reaction side, the remaining material was washed, and the solution was filtered again. Crystallization of the sample was carried out (see description above). Colorless crystals (1.014 g, 0.91 mmol, 91 % yield) very sensitive to air and moisture were isolated and characterized by NMR (CD_2Cl_2): ^{19}F-NMR: $\delta = -75.7$ ppm (s, 36F), ^{27}Al-NMR: $\delta = 31.9$ ppm (s, 1Al), $^{13}C\{^1H\}$-NMR: $\delta = 110.0$ ppm (s, 6C), $\delta = 122.0$ ppm (q, 16C, $^1J_{C\text{-}F} = 294.4$ Hz). ^{1}H-NMR: $\delta = 5.47$ ppm (s, 12H), IR (CsI-Plates, Nujol): ν [cm^{-1}] = 445 (mw), 537 (mw), 562 (mw), 612 (w), 652 (vw), 668 (w), 727 (s), 757 (w), 833 (mw), 973 (vs), 1006 (mw), 1162 (m), 1216 (vs), 1244 (s), 1275 (vs), 1301 (s), 3118 (vw) and Raman spectroscopy [cm^{-1}/ (%)]: 3147(6), 3096(19), 3045(4), 3013(100), 1577(65), 1483(2), 1321(78), 1009 (29), 495(6), and X-ray single crystal structure.

Diagram of the Schlenk glassware implemented for the reactions.

One of the advantages of such a system over “standard” Schlenk flasks is the absence of grease for the taps. Furthermore, the reaction mixture once inside, can be treated until purification without opening the valves; therefore a minimization of air and moisture is reached. Low temperature crystallization (below 0°C) can be easily achieved if the J. Young taps used are made of glass. Teflon taps are suitable for reaction and crystallization procedures above 0°C.

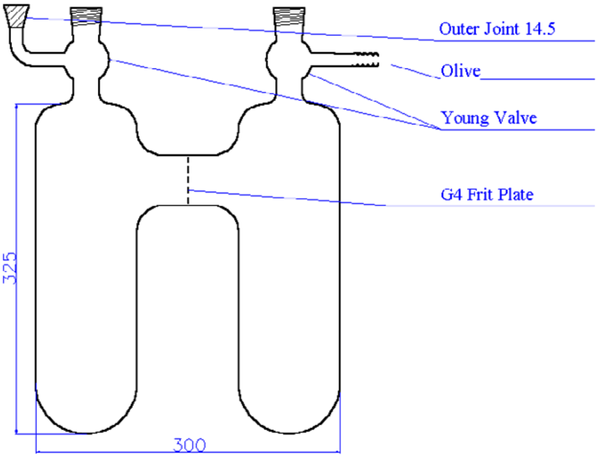

Notes and References for supplemental material

s.1 H.-C. Tai, I. Krossing, M. Seth, D. V. Deubel, *Organometallics* **2004**, *23*,2343.

s.2 D. R. Lide. *CRC-Handbook of Chemistry and Physics*. *83rd ed.* **2002-2003**, CRC Press, Florida, U.S.A.

s.3 A. F. Holleman, N. Wiberg. *Lehrbuch der Anorg. Chem.* 101 Auflage. Walter de Gruyter&Co, Berlin, **1995**. 2033 pp.

s.4 **a)** Ph. D. thesis: A. Reisinger. **2007**. Albert-Ludwig Universität Freiburg. **b)** Paper submitted to *J. Am. Chem. Soc*, **2007.**

s.5 National Institute of Standards ant Technology, http://www.nist.gov.

s.6 H-C. Tai, I. Krossing, M. Seth, D. V. Deubel. *Organometallics*, **2004**, *23*, 2343-2349.

s.7 **a)** I. Krossing. *J. Am. Chem. Soc*. **2001**, *123*, 4603-4604. **b)** I. Krossing, L. Van Wüllen. *Chem. Eur. J.* **2002**, *8*, 700-711.

s.8 I. Krossing. *Chem. Eur. J.* **2001**, *7*, 490-502.